Domain Formation in Sphingomyelin/Cholesterol Mixed Membranes Studied by Spin-Label Electron Spin Resonance Spectroscopy†

M. Isabel Collado,‡ Félix M. Goñi,‡ Alicia Alonso,‡ and Derek Marsh*,§

Max-Planck-Institut für biophysikalische Chemie, Abteilung Spektroskopie, 37070 Göttingen, Germany, and Unidad de Biofísica (CSIC−UPV/EHU) and Departamento de Bioquímica, Universidad del País Vasco, Apartado 644, E-48080 Bilbao, Spain

Received November 29, 2004; Revised Manuscript Received January 28, 2005

ABSTRACT: Interactions of palmitoylsphingomyelin with cholesterol in multilamellar vesicles have been studied over a wide range of compositions and temperatures in excess water by using electron spin resonance (ESR) spectroscopy. Spin labels bearing the nitroxide free radical group on the 5 or 14 C-atom in either the *sn*-2 stearoyl chain of phosphatidylcholine (predominantly 1-palmitoyl) or the *N*-stearoyl chain of sphingomyelin were used to determine the mobility and ordering of the lipids in the different phases. Two-component ESR spectra of the 14-position spin labels demonstrate the coexistence first of gel (L_β) and liquid-ordered (L_o) phases and then of liquid-ordered and liquid-disordered (L_α) phases, with progressively increasing temperature. These phase coexistences are detected over a limited range of cholesterol contents. ESR spectra of the 5-position spin labels register an abrupt increase in ordering at the $L_\alpha-L_o$ transition and a biphasic response at the $L_\beta-L_o$ transition. Differences in outer splitting between the C14-labeled sphingomyelin and phosphatidylcholine probes are attributed to partial interdigitation of the sphingomyelin *N*-acyl chains across the bilayer plane in the L_o state. In the region where the two fluid phases, L_α and L_o, coexist, the rate at which lipids exchange between phases ($\ll 7 \times 10^7\ s^{-1}$) is much slower than translational rates in the L_α phase, which facilitates resolution of two-component spectra.

Sphingomyelin (SM)[1] and cholesterol (Chol) are major components of the plasma membrane outer leaflet in mammals. The "raft hypothesis" (*1*) brought these lipids into prominence because assemblies of sphingolipids and cholesterol were proposed to function as platforms for specific membrane proteins. This hypothesis revived an interest in past investigations on SM/Chol interactions and promoted a series of new ones. SM/Chol mixtures had been studied by Sankaram and Thompson (*2*), who described a partial phase diagram for bilayers in the fluid state and proposed that cholesterol would induce formation of a "liquid-ordered" (L_o) phase that would initially coexist with the liquid-crystalline L_α phase and, beyond a given cholesterol concentration (≈20 mol % or higher), become predominant. The L_o phases had previously been described theoretically by Ipsen et al. (*3*) as liquid-crystalline phases with a high acyl-chain order. The earlier studies have been discussed in a series of recent reviews on cholesterol/phospholipid interactions, the liquid-ordered phase, and lipid rafts (*4*−*10*).

Among the more recent work, several authors have carried out biophysical studies on ternary systems intended to represent an ideal "raft mixture", i.e., phosphatidylcholine (PC), SM, and Chol. Dietrich et al. (*11*) were able to observe L_o/L_α phase coexistence in giant unilamellar vesicles composed of PC, SM, and Chol and containing fluorescent probes. Rinia et al. (*12*), using atomic force microscopy, visualized phase separation in supported lipid bilayers also consisting of PC, SM, and Chol. Aussenac et al. (*13*) applied ^2H and ^{31}P solid-state NMR to the detection of L_o phases in ternary and quaternary raft mixtures, while Veatch et al. (*14*) combined NMR and fluorescence microscopy to detect liquid−liquid immiscibility in dioleoyl-PC, dipalmitoyl-PC, and Chol bilayers. Importantly, de Almeida et al. (*15*) were able to construct a detailed ternary phase diagram for palmitoyl-SM, palmitoyloleoyl-PC and Chol, based mainly on fluorescence measurements.

SM/Chol binary mixtures have been studied with a variety of techniques. Mannock et al. (*16*) used differential scanning calorimetry and other techniques to show the ability of cholesterol to increase the width, decrease the enthalpy, and eventually smear out the gel−fluid transition of sphingomyelin, observations in agreement with previous ones by Estep et al. (*17*, *18*) and Maulik and Shipley (*19*) and later ones by Contreras et al. (*20*). Whether sphingomyelin and cholesterol give rise, or not, to specific complexes is a debated issue, with data that seem to favor this hypothesis (*21*−*24*) and data that appear to contradict it (*16*, *25*−*28*). The possibility of coexisting lipid−lipid domains in binary SM/Chol mixtures has been examined by various authors. Radakrishnan et al. (*22*) and previously Slotte (*29*) observed liquid−liquid immiscibility in mixed SM/Chol monolayers,

† This work was supported in part by grants from DGICYT (Spain) (BMC 2002-00784) and from the University of the Basque Country (9/UPV 00042.310-13552/2001).

* Corresponding author. Tel: +49-551-201 1285. Fax: +49-551-201 1501. E-mail: dmarsh@gwdg.de.

‡ Universidad del País Vasco.

§ Max-Planck-Institut für biophysikalische Chemie.

[1] Abbreviations: *n*-SMSL, *N*-[*n*-(4,4-dimethyloxazolidine-*N*-oxyl)-stearoyl]sphingosine-1-phosphocholine; *n*-PCSL, 1-acyl-2-[*n*-(4,4-dimethyloxazolidine-*N*-oxyl)stearoyl]-*sn*-glycero-3-phosphocholine; C16-SM, *N*-palmitoylsphingosine-1-phosphocholine; SM, sphingomyelin; PC, phosphatidylcholine; Chol, cholesterol; Hepes, *N*-(2-hydroxyethyl)-piperazine-*N*′-2-ethanesulfonic acid; EDTA, ethylenediaminetetraacetic acid; ESR, electron spin resonance; L_α, fluid (liquid-disordered) lamellar phase; L_β, lamellar gel phase; L_o, liquid-ordered lamellar phase.

10.1021/bi0474970 CCC: $30.25
Published on Web 03/05/2005

but only at lateral pressures ≤20 mN m^{-1}, i.e., well below those estimated for cell membranes (≥30 mN m^{-1}) (*30*). NMR studies on SM/Chol mixtures have been interpreted in terms of rapid lipid exchange between assumed coexisting liquid-ordered and liquid-disordered phases. Guo et al. (*27*) used solid-state NMR while Filippov et al. (*31*) applied pulsed field gradient NMR to mixtures of cholesterol and sphingomyelin of natural origin. In the latter study, average translational diffusion coefficients were found to conform with the Gibbs phase rule. The region of phase coexistence was found to lie between ≈5 and 25 mol % Chol (*31*), in agreement with the early ESR observations by Sankaram and Thompson (*2*). Direct visualization of fluid−fluid-phase coexistence in membranes composed of binary lipid mixtures with cholesterol, e.g., by fluorescence microscopy or two-component spectra, however, has so far proved difficult.

Previous joint studies from our laboratories include ESR investigations of binary (sphingolipids plus glycerolipids) and ternary (sphingolipids plus glycerolipids plus Chol) mixtures, using both spin-labeled PC and SM as probes. Mixtures of sphingolipids and glycerolipids of natural origin (*32*) showed good mixing above the gel-to-fluid transition of the sphingolipids, while gel and fluid phases coexisted below this transition. When cholesterol was included in the bilayers (*23*), formation of the L_o phase was detected, concomitant with partial transbilayer interdigitation of the sphingomyelin *N*-acyl chains. Cholesterol-induced interdigitation was suggested to stabilize the coexistence of gel-phase and L_o domains.

The present work is intended to explore domain formation in SM/Chol mixed membranes by using ESR spectroscopy. The combined use of SM and PC probes, the former known to exhibit a preference for the L_o phase in ternary mixtures (*23*), together with an extensive range of temperatures and cholesterol concentrations, will provide a detailed view of this system. In addition, the use of a chemically homogeneous (*N*-palmitoyl) species of sphingomyelin is intended to better define the phase behavior. Our results provide examples not only of the coexistence of gel plus L_o phases at lower temperatures but also of L_α plus L_o phases (i.e., fluid−fluid-phase separation) at higher temperatures.

MATERIALS AND METHODS

Materials. N-Palmitoylsphingomyelin (C16-SM) was from Avanti Polar Lipids (Alabaster, AL). Cholesterol was from Sigma Chemical Co. (St. Louis, MO). Phosphatidylcholine spin labels labeled at C5 or C14 in the stearoyl *sn*-2 chain of the lipid were synthesized as described earlier by acylation of lysophosphatidylcholine (predominantly palmitoyl) from egg yolk (*33*). Sphingomyelin spin labels labeled at the C5 or C14 positions in the *N*-acyl chain were synthesized by the coupling reaction of the *N*-succinimidyl ester of spin-labeled stearic acid (*34*) with sphingosine-1-phosphocholine derived from bovine brain sphingomyelin (*35*).

Sample Preparation. For ESR measurements, 2 μmol of total lipids and 0.5 mol % spin label were codissolved in chloroform or chloroform−methanol (2:1 v/v) and evaporated under a stream of dry nitrogen gas. The residual solvent was removed by vacuum-drying overnight. The lipid film was then hydrated in 0.1 mL of 20 mM Hepes, 100 mM NaCl, and 1 mM EDTA, pH 7.4, by incubation for 1 h at 50 °C with vortexing. Samples were then pelleted into a 1 mm inside diameter (i.d.) glass capillary, the excess supernatant was removed, and the capillary was flame sealed.

ESR Measurements. ESR spectra were recorded on a Varian Century Line 9 GHz spectrometer equipped with nitrogen gas-flow temperature regulation. Samples in 1 mm i.d. glass capillaries were placed in a standard quartz ESR tube containing light silicone oil for thermal stability. Spectral data were collected digitally on a personal computer using software written by Dr. M. D. King. Outer hyperfine splittings ($2A_{max}$) were used to characterize the rotational disorder and rotational rates of the spin-labeled lipid chain segments (see, e.g., refs *36* and *37*). For rotational mobility with components in the slow-motional regime (*38*), this parameter provides a useful comparative indicator of segmental mobility in equivalent systems (e.g., ref *39*). Spectral subtractions were performed as described previously (*40*) using interactive graphics software written by Dr. J.-H. Kleinschmidt. Where necessary, small corrections were made for any residual second component in the experimental spectra used as "single" components for subtraction.

RESULTS

The chain-melting transition of C16-sphingomyelin membranes not containing cholesterol occurs at ca. 41 °C (*19*). Systematic spectroscopic investigations of the dependence on cholesterol content were carried out at different temperatures corresponding to the gel (L_β) and fluid (L_α) phases of pure C16-SM bilayer membranes. For the mixtures, this includes also the liquid-ordered (L_o) phase of the cholesterol-containing membranes.

ESR spectra of samples at lower temperature, in the gel and liquid-ordered phases, are considered first. This is then followed by consideration of samples at higher temperature that are in the liquid-disordered (i.e., L_α) or liquid-ordered phases. In each case, ESR spectra from sphingomyelin and phosphatidylcholine spin-labeled on the 14 C-atom of the *N*-acyl, or *sn*-2, chain are presented first. These labels are best able to detect phase coexistence, because the spectral differences between the more ordered and less ordered phases are greatest for spin labels positioned closer to the terminal methyl end of the acyl chain (see, e.g., refs *32* and *41*). Spectra from sphingomyelin and phosphatidylcholine spin-labeled at the 5 C-atom of the *N*-acyl, or *sn*-2, chain are presented afterward. Spectra at this position of chain labeling are most sensitive to the dependence of chain ordering on cholesterol content in single phases. Use of two different phospholipid probe species (SM and PC) helps to establish the generality of conclusions on phase coexistence that are deduced from the ESR spectra.

Gel and Liquid-Ordered Phases: 14-Position Spin Labels. Figure 1 shows the ESR spectra of the 14-PCSL phosphatidylcholine spin label in hydrated mixtures of C16-SM and cholesterol at temperatures of 22 and 30 °C, which correspond to the gel phase of pure C16-SM bilayers. At 22 °C, the ESR spectra of 14-PCSL very clearly consist of two components, for samples with cholesterol contents in the range 12.5−20 mol %. The spectral component with larger outer hyperfine splitting (see Figure 1, left-hand panel) corresponds to gel-phase regions (L_β), and that with the smaller outer hyperfine splitting corresponds to regions of

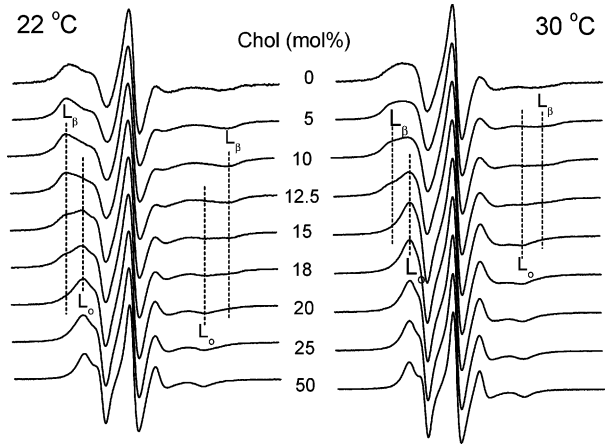

FIGURE 1: ESR spectra of 14-PCSL, spin-labeled phosphatidylcholine, in hydrated bilayer membranes of palmitoylsphingomyelin (C16-SM) containing cholesterol. The cholesterol content is indicated in the figure. Dashed vertical lines indicate the outer splittings, $2A_{max}$, of the two coexisting spectral components arising from the gel (L_β) and liquid-ordered (L_o) phases. Left-hand panel: samples at 22 °C. Right-hand panel: samples at 30 °C. Total scan width: 100 G.

liquid-ordered phase (L_o). With increasing content of cholesterol, the proportion of the L_o component increases at the expense of the gel-phase component.

At the higher temperature of 30 °C, the spectra of 14-PCSL again correspond to two components, at certain cholesterol contents (see Figure 1, right-hand panel). Relative to 22 °C (Figure 1, left-hand panel), the coexistence region of the two spectral components is shifted to lower cholesterol contents, approximately in the range 5−15 mol % cholesterol.

Similar experiments have also been performed with the 14-SMSL sphingomyelin spin label. The two spectral components corresponding to gel and L_o phases are not resolved with this particular label (data not shown). The difference from the 14-PCSL spin label arises from the different backbone attachments of the sphingolipid *N*-acyl chain and the glycerolipid *sn*-2 chain and their lengths relative to the sphingosine and *sn*-1 chains, respectively. This results in the spectra of 14-SMSL being very similar in the gel and liquid crystalline phases (see ref *32*).

Figure 2 shows the dependence on cholesterol concentration of the outer hyperfine splitting, $2A_{max}$ (see Figure 1 for definition), for both 14-PCSL and 14-SMSL spin labels, in mixtures with C16-sphingomyelin. Data in the different panels correspond to different sample temperatures. In panel A, double-valued entries for 14-PCSL represent the range of cholesterol contents over which gel and L_o phases coexist (demarcated by the vertical dashed lines). Similar coexistence is observed at 27 and 30 °C, but at lower cholesterol contents (see Figure 1), and is indicated by the vertical dashed lines in panel B. In the absence of resolved coexisting spectra for 14-SMSL, the effective outer hyperfine splitting, $2A_{max}$, nonetheless decreases sharply in this region.

Figure 3 resolves the two spectral components from 14-PCSL in a C16-SM membrane containing 18 mol % cholesterol at 22 °C by using spectral subtraction. Subtracting a spectrum from C16-SM plus 25 mol % Chol membranes at 22 °C yields a single-component spectral line shape that closely resembles that from C16-SM plus 10 mol % Chol

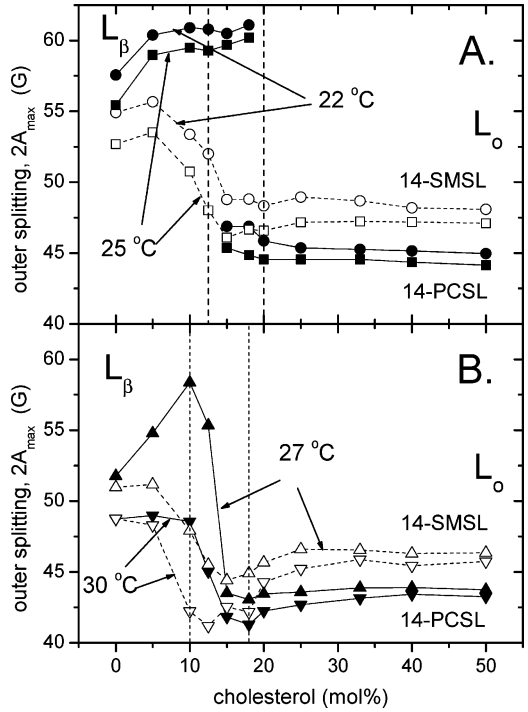

FIGURE 2: Dependence on cholesterol content of the outer hyperfine splitting, $2A_{max}$, of the 14-PCSL (solid symbols, solid lines) and 14-SMSL spin labels (open symbols, dashed lines) in hydrated C16-sphingomyelin bilayer membranes. The different panels correspond to different sample temperatures, as indicated on the figure. (A) 22 °C (●, ○) and 26 °C (■, □). (B) 27 °C (▲, △) and 30 °C (▼, ▽). Typical uncertainty in $2A_{max}$ is ±0.2−0.4 G.

membranes at 22 °C, and vice versa. Figure 4 shows that, quantitatively, the fractional population, *f*, of spin-labeled lipid in the liquid-ordered phase, for a membrane with mole fraction *X* of cholesterol, follows the lever rule (*42*):

$$f = \frac{X - X_S}{X_F - X_S} \quad (1)$$

where X_S is the mole fraction of cholesterol in the gel-phase domains (S ≡ L_β) and X_F that in the liquid-ordered phase domains (F ≡ L_o). The linearity of the dependence on cholesterol content in Figure 4 implies that the 14-PCSL probe partitions approximately equally between the gel and liquid-ordered phases. The phase boundaries deduced from fitting eq 1 to the dependence of *f* on cholesterol concentration are given in the inset to Figure 4.

Gel and Liquid-Ordered Phases: 5-Position Spin Labels. The left-hand panel of Figure 5 shows the ESR spectra of the 5-PCSL phosphatidylcholine spin label in C16-SM plus cholesterol mixed membranes at 30 °C. The outer hyperfine splitting (indicated by the dashed lines on the figure) is large, characteristic of a low-mobility and/or highly ordered state. The spectral line shapes remain rather similar up to 12.5 mol % cholesterol. At 15 and 18 mol % cholesterol, the spectra are characteristic of a somewhat more mobile state. Beyond this, the spectra display evidence of increasing chain order, i.e., larger hyperfine splitting and sharper lines, with increasing cholesterol content. (In the high cholesterol regime, there is evidence of slightly decreasing order; see below.) Essentially similar, although less pronounced, changes are recorded by the 5-SMSL sphingomyelin spin label (Figure 5, right-hand panel).

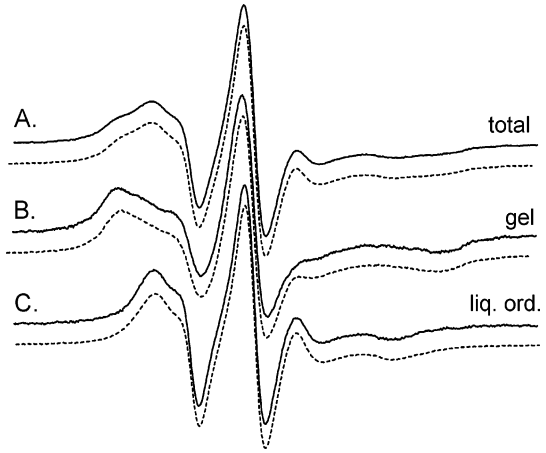

FIGURE 3: Difference spectroscopy for 14-PCSL in C16-SM/18 mol % cholesterol membranes at 22 °C. (A) Solid line, original spectrum; dashed line, sum from 57% of the dashed spectrum in (B) and 43% of that in (C). (B) Solid line, gel-phase difference spectrum resulting from subtracting 43% of the dashed spectrum in (C) from the original spectrum in (A); dashed line, gel-phase reference spectrum (C16-SM/10 mol % Chol at 22 °C). (C) Solid line, liquid-ordered difference spectrum resulting from subtracting 57% of the dashed spectrum in (B) from the original spectrum; dashed line, liquid-ordered phase reference spectrum (C16-SM/25 mol % Chol at 22 °C). Percentages in each case refer to the double-integrated intensities of the first-derivative spectra. Scan range = 100 G.

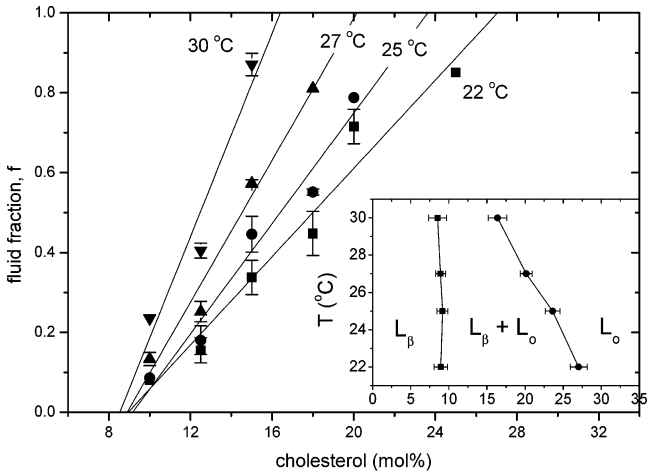

FIGURE 4: Dependence on cholesterol content of the fraction *f* of the liquid-ordered component in the spectra from 14-PCSL in C16-SM/Chol mixed membranes at the temperatures indicated. Solid lines are least-squares fits of eq 1. Inset: Boundaries for onset (squares) and completion (circles) of gel (L_β)/liquid-ordered (L_o) phase separation deduced from the linear fits.

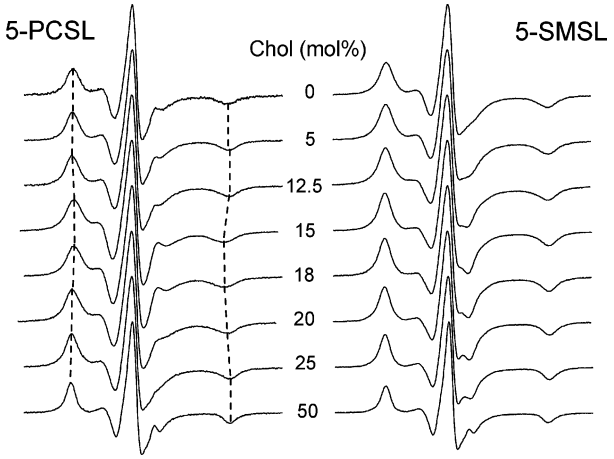

FIGURE 5: ESR spectra of 5-PCSL (left-hand panel) and 5-SMSL (right-hand panel) in hydrated bilayer membranes of C16-SM. The cholesterol content is indicated on the figure. $T = 30$ °C; total scan width = 100 G.

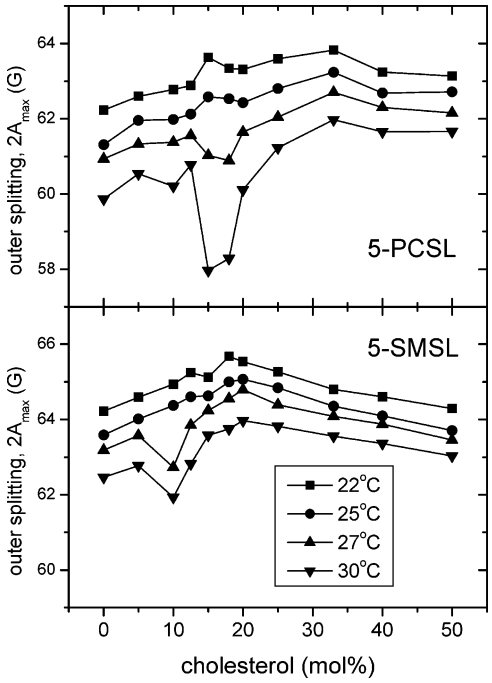

FIGURE 6: Dependence on cholesterol content of the outer hyperfine splitting, $2A_{max}$, of the 5-PCSL (upper panel) and 5-SMSL (lower panel) spin labels in hydrated C16-SM membranes. The different sample temperatures are indicated on the figure. Typical uncertainty in $2A_{max}$ is $\pm 0.2-0.4$ G.

Figure 6 shows the dependence of the outer hyperfine splittings, $2A_{max}$, of the 5-PCSL and 5-SMSL spin label on cholesterol content of the C16-SM mixed membranes, at various temperatures in the lower range. The responses are biphasic in the transition region and multiphasic over the whole range, depending on ordering effects, fluidizing effects, and (unresolved) phase coexistence in the different regimes of cholesterol content.

Liquid-Disordered and Liquid-Ordered Phases: 14-Position Labels. The left-hand panel of Figure 7 shows the ESR spectra of the 14-PCSL phosphatidylcholine spin label in C16-SM plus cholesterol membranes at 50 °C. In the absence of cholesterol, 14-PCSL displays a quasi-isotropic, sharp three-line, single-component spectrum that is characteristic of the fluid L_α phase. With 50 mol % cholesterol, the ESR spectrum of 14-PCSL consists of a single axially anisotropic component with dynamics characteristic of the liquid-ordered L_o phase. At intermediate cholesterol contents, viz., 20 mol %, the spectra consist of two components that are characteristic of coexisting liquid-disordered and liquid-ordered phases. These two spectral components are indicated by the dashed vertical lines in the high-field region of the spectra in Figure 7. Spectral subtraction (data not shown) reveals coexisting spectral components over the approximate range from 12.5 to 20 mol % cholesterol. Phase boundaries for the L_α and L_o regions at 50 °C are predicted at approximately 10 ± 1 and 24 ± 1 mol % cholesterol, respectively, by using the method of Figure 4.

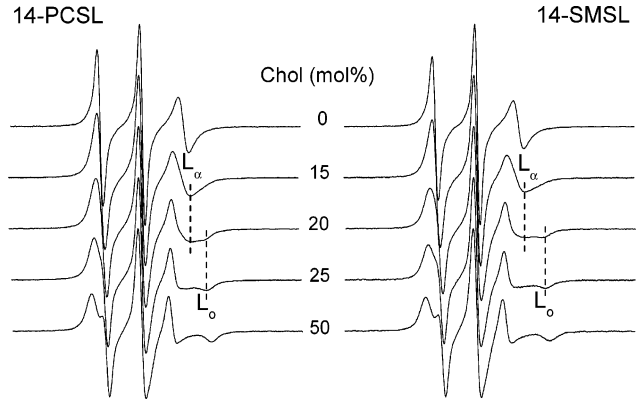

FIGURE 7: ESR spectra of 14-PCSL (left-hand panel) and 14-SMSL (right-hand panel) spin labels in hydrated bilayer mixed membranes of C16-SM and cholesterol at 50 °C. The cholesterol content is indicated on the figure. The dashed vertical lines indicate the high-field peaks of the coexisting spectral components from the liquid-disordered (L_α) and liquid-ordered (L_o) phases. Total scan width: 100 G.

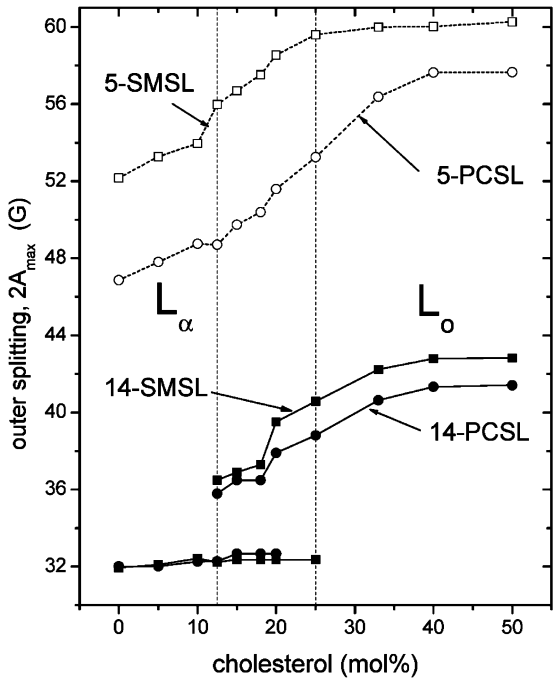

FIGURE 8: Dependence on cholesterol content of the outer hyperfine splittings of the 14-PCSL and 14-SMSL spin labels in hydrated C16-SM membranes (solid lines and symbols) at 50 °C. Corresponding data for the 5-PCSL and 5-SMSL spin labels are given by dashed lines and open symbols. Typical uncertainty in $2A_{max}$ is ±0.2−0.4 G.

The right-hand panel of Figure 7 shows the corresponding spectra of the 14-SMSL sphingomyelin spin label. A very similar picture emerges to that obtained with the 14-PCSL spin label. Two coexisting spectral components are obtained from the sample with 20 mol % cholesterol, for example. It is noted that, in contrast to the situation with L_β−L_o phase coexistence, two spectral components are observed with 14-SMSL in the region of L_α−L_o coexistence because the outer hyperfine splitting of 14-SMSL in the presence of cholesterol is larger than that for 14-PCSL (see Figure 2 and ref *23*).

Figure 8 shows the dependence on cholesterol content of the outer hyperfine splitting, $2A_{max}$, of both 14-PCSL and 14-SMSL in membranes at 50 °C. The region of coexistence

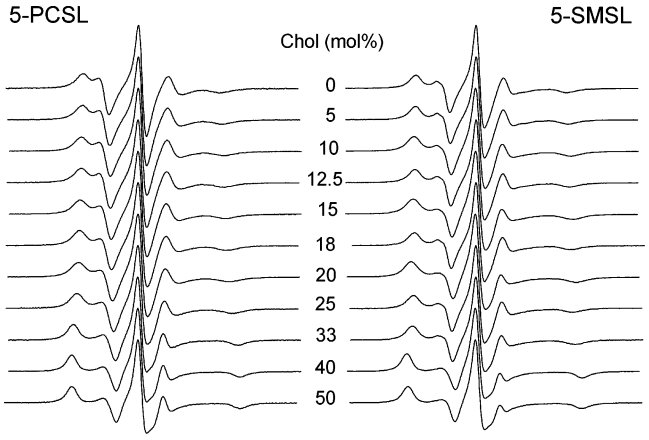

FIGURE 9: ESR spectra of 5-PCSL (left-hand panel) and 5-SMSL (right-hand panel) spin labels in C16-SM/cholesterol membranes at 50 °C. The cholesterol content is indicated on the figure. Total scan width: 100 G.

of liquid-disordered (L_α) and liquid-ordered (L_o) phases (i.e., of two-component spectra) is indicated by the double-valued entries and approximately by the vertical dashed lines. Outside this range, $2A_{max}$ increases with increasing cholesterol content in the L_o single-phase region but displays relatively little cholesterol dependence (at this label position) in the L_α-phase region.

Liquid-Disordered and Liquid-Ordered Phases: 5-Position Spin Labels. Figure 9 (left-hand panel) shows the ESR spectra of the 5-PCSL spin label in hydrated C16-SM membranes at 50 °C as a function of cholesterol content. All spectra consist of apparently single-component, axially anisotropic powder patterns that are characteristic of fluid phases. The spectral anisotropy measured by the difference in the splittings between the outer and inner peaks increases progressively with increasing cholesterol content in the membranes.

The right-hand panel of Figure 9 shows the corresponding ESR spectra of the 5-SMSL sphingomyelin spin label. Again, as for 5-PCSL, the spectra are all apparently single-component, axially anisotropic powder patterns. The outer hyperfine splitting at 50 °C, as a function of cholesterol content, is given for both 5-position spin labels (as for the 14-position labels), also in Figure 8. The steepest part of the functional dependence corresponds to the region of phase coexistence that is detected by the 14-position spin labels.

DISCUSSION

The ESR results reported here provide essential information on the phase behavior and lipid chain ordering in membranes of C16-SM/cholesterol mixtures. Undoubtedly the most significant result is the direct demonstration of the coexistence of sphingolipid-containing liquid-ordered and liquid-disordered phases that is presented in Figure 7. Whereas the coexistence of gel and liquid-ordered phases has been demonstrated previously for glycerolipids by ^{2}H NMR spectroscopy (*43*), and later for sphingolipids by ^{2}H NMR (*44*), and further by ESR spectroscopy for complex sphingolipid/glycerolipid mixtures (*23*), a direct visualization of the coexistence of liquid-ordered and liquid-disordered phases, i.e., fluid−fluid-phase separation, spectroscopically in two-component bilayer membranes has proved rather elusive (cf. also ref *45*).

The features of the various cholesterol-containing sphingolipid phases and their coexistence that are deduced from the ESR spectra of the C-14 and C-5 position spin-labeled lipids are discussed below. The lower temperature regime (L_β and L_o) is treated first, followed by the higher temperature regime (L_α and L_o).

Gel−Liquid-Ordered ($L_\beta-L_o$) Coexistence. The two-component spectra of the 14-PCSL spin label (Figure 1) graphically demonstrate the coexistence of gel and liquid-ordered phases. Spectral subtraction (Figure 3) shows that the individual spectral line shapes of the two components do not change throughout the two-phase region, as is required by the Gibbs phase rule. Figures 2 and 4 show that the region of phase coexistence moves to lower cholesterol concentrations and decreases in width, as the temperature is increased toward the chain-melting temperature of C16-SM alone. This is in good agreement with the partial phase diagram for C16-SM/cholesterol that was published by de Almeida et al. (*15*), based on fluorescence spectroscopy. Qualitatively, the cholesterol dependence of the outer splitting from the 14-SMSL sphingomyelin spin label (see Figure 2) is in agreement with this interpretation of the phase mixing behavior in this part of the binary phase diagram, although two-component spectra are not resolved directly (see also ref *32*).

In this region of the phase diagram, i.e., at relatively low temperatures, the outer hyperfine splittings of the 5-position spin labels are all large (see Figure 5) and sensitive both to rotational rates (in the slow motional regime) and to amplitudes of motion (in the high-ordering regime). Initial admixture of cholesterol at low concentrations causes either little effect or a slight ordering of the gel phase, depending on temperature (see Figure 6). Beyond this point, a disordering or fluidizing effect that corresponds to formation of the liquid-ordered phase takes place at 27 and 30 °C. This is observed at 12.5−15 mol % cholesterol with 5-PCSL and at 5−10 mol % cholesterol with 5-SMSL (cf. Figure 2). Beyond the two-phase region of $L_\beta-L_o$ coexistence, further ordering of the 5-PCSL spin label takes place in the single-phase liquid-ordered region, although this is not registered by the 5-SMSL spin label. Finally, a decrease in effective ordering is observed with both 5-PCSL and 5-SMSL, at the highest cholesterol contents.

Chain Interdigitation in the L_o Phase. Figure 2 shows that in the gel phase of C16-SM, in the absence of cholesterol, the outer hyperfine splitting of 14-SMSL is less than that of 14-PCSL. In the liquid-ordered phase, at cholesterol contents above 20 mol %, however, this situation is reversed. The result for the gel phase is explained by reference to the crystal structure of glycerolipids and sphingolipids (see ref *32*). The spin-labeled *sn*-2 chain of phosphatidylcholine is overlapped completely by the *sn*-1 chain, whereas the spin-labeled *N*-acyl chain of sphingomyelin is longer than the sphingosine chain. This lack of interchain overlap at the C-14 position of the *N*-acyl chain accounts for the smaller outer splitting of 14-SMSL in the gel phase. Correspondingly, the larger outer splitting of 14-SMSL, relative to 14-PCSL, in the L_o phase can be attributed to a partial interdigitation of the spin-labeled *N*-acyl chain from sphingomyelin across the bilayer midplane. This effect has been observed previously in mixtures of cholesterol with sphingolipids of natural origin (*23*). Transbilayer interdigitation of *N*-acyl chains from sphingolipids in the exoplasmic leaflet that is induced by the presence of cholesterol in the cytoplasmic leaflet has been proposed as a mechanism for stabilization of sphingolipid "rafts" in cell membranes (*1*).

Liquid-Disordered/Liquid-Ordered ($L_\alpha-L_o$) Coexistence. Compared with the gel/L_o-phase coexistence, information on $L_\alpha-L_o$ boundaries in lipid/cholesterol binary phase diagrams is scarcer, less precise, and based mostly on indirect measurements (*2*, *15*, *43*). Detection of small domains depends on the time scale of the spectroscopic technique, or on the spatial resolution of the microscopy, that is used for observation. Direct visualization of liquid-ordered/liquid-disordered phase coexistence in bilayer membranes has so far been restricted to studies with a biradical spin label in glycerolipid systems (*46*). Recent imaging of coexisting fluid domains by two-photon microscopy of giant vesicles is confined to cholesterol-containing ternary lipid systems (*11*, *47*). Visualization of fluid−fluid-phase separation by fluorescence microscopy has not proved possible in binary mixtures of cholesterol with a single lipid (*45*, *48*). The unambiguous demonstration here of coexistence between fluid domains with high and low cholesterol content in sphingomyelin membranes therefore adds significant experimental support to the theoretical prediction of the existence of a liquid-ordered phase that is distinct from the fluid L_α phase in lipid mixtures with cholesterol (*3*). More specifically, it points to the potential physiological relevance of liquid-ordered phases of sphingolipids in cell membranes.

A feature of considerable interest is the rate at which lipids exchange between the two fluid phases, L_o and L_α. In the region where two-component spectra are resolved (see Figure 7), the exchange is slow compared with the separation, δH, of the high-field peaks from the 14-position labels in the L_α and L_o domains. For the spectra in Figure 7, this corresponds to frequencies in the region of $g_e\beta_e\delta H/\hbar \approx 7 \times 10^7\ s^{-1}$. Therefore, the exchange rate must be considerably slower than the translational diffusion rates in L_α phases (*49*), as is necessary to maintain phase separation between fluid domains.

Outer hyperfine splittings of the 14-position spin labels at 50 °C indicate very clearly the increase in lipid chain ordering on formation of the liquid-ordered phase (see Figure 8). At this position of the chain, the dependence of ordering on cholesterol content in the single-phase regions is greater for the liquid-ordered phase than for the liquid-disordered phase. Changes in spin-label outer hyperfine splitting at the C-5 position of the chain show a greater dependence on cholesterol than do those at the C-14 position (see Figure 8). Because the overall order is greater at the C-5 position of the chain, separate spectral components are not resolved in the phase coexistence region (see Figure 9). Varying proportions of the two unresolved components then cause the change in A_{max} with cholesterol content in the two-phase regime. In contrast to the situation with the 14-position labels, chain ordering at the C-5 segments displays a pronounced dependence on cholesterol content in both L_α and L_o single-phase regions.

CONCLUSIONS

The experimental data presented in this paper demonstrate that, for lipid bilayers consisting of palmitoyl-SM and Chol in multilamellar vesicles in excess water, gel and L_o phases

coexist at temperatures up to at least 30 °C, i.e., below the gel−fluid transition of palmitoyl-SM (41 °C). At higher temperatures, i.e., 50 °C, coexistence of the L_α and L_o fluid phases is observed. Under these conditions, phase separation is maintained due to a slow rate of interdomain lipid exchange. In addition, interdigitation of SM acyl chains across the bilayer mid-plane occurs in the L_o phase. Taken together, these observations provide a detailed description of the phenomena of L_α−L_o coexistence in a two-lipid system and may contribute to our understanding of the physical basis of lipid domain formation in (fluid) cell membranes.

ACKNOWLEDGMENT

We thank Frau B. Angerstein for synthesis of spin-labeled lipids.

REFERENCES

1. Simons, K., and Ikonen, E. (1997) Functional rafts in cell membranes, *Nature 387*, 569−572.
2. Sankaram, M. B., and Thompson, T. E. (1990) Interaction of cholesterol with various glycerophospholipids and sphingomyelin, *Biochemistry 29*, 10670−10675.
3. Ipsen, J. H., Karlstrom, G., Mouritsen, O. G., Wennerstrom, H., and Zuckermann, M. J. (1987) Phase equilibria in the phosphatidylcholine-cholesterol system, *Biochim. Biophys. Acta 905*, 162−172.
4. McConnell, H. M., and Vrljic, M. (2003) Liquid−liquid immiscibility in membranes, *Annu. Rev. Biophys. Biomol. Struct. 32*, 469−492.
5. Silvius, J. R. (2003) Role of cholesterol in lipid raft formation: lessons from lipid model systems, *Biochim. Biophys. Acta 1610*, 174−183.
6. Allende, D., Vidal, A., and McIntosh, T. J. (2004) Jumping to rafts: gatekeeper role of bilayer elasticity, *Trends Biochem. Sci. 29*, 325−330.
7. Barenholz, Y. (2004) Sphingomyelin and cholesterol: from membrane biophysics and rafts to potential medical applications, *Subcell. Biochem. 37*, 167−215.
8. McMullen, T. P. W., Lewis, R. N. A. H., and McElhaney, R. N. (2004) Cholesterol-phospholipid interactions, the liquid-ordered phase and lipid rafts in model and biological membranes, *Curr. Opin. Colloid Interface Sci. 8*, 459−468.
9. Oradd, G., and Lindblom, G. (2004) Lateral diffusion studied by pulsed field gradient NMR on oriented lipid membranes, *Magn. Reson. Chem. 42*, 123−131.
10. Simons, K., and Vaz, W. L. (2004) Model systems, lipid rafts, and cell membranes, *Annu. Rev. Biophys. Biomol. Struct. 33*, 269−295.
11. Dietrich, C., Bagatolli, L. A., Volovyk, Z. N., Thompson, N. L., Levi, M., Jacobson, K., and Gratton, E. (2001) Lipid rafts reconstituted in model membranes, *Biophys. J. 80*, 1417−1428.
12. Rinia, H. A., Snel, M. M. E., van der Eerden, J. P. J. M., and De Kruijff, B. (2001) Visualizing detergent resistant domains in model membranes with atomic force microscopy, *FEBS Lett. 501*, 92−96.
13. Aussenac, F., Tavares, M., and Dufourc, E. J. (2003) Cholesterol dynamics in membranes of raft composition: a molecular point of view from ^{2}H and ^{31}P solid-state NMR, *Biochemistry 42*, 1383−1390.
14. Veatch, S. L., Polozov, I. V., Gawrisch, K., and Keller, S. L. (2004) Liquid domains in vesicles investigated by NMR and fluorescence microscopy, *Biophys. J. 86*, 2910−2922.
15. de Almeida, R. F. M., Fedorov, A., and Prieto, M. (2003) Sphingomyelin/phosphatidylcholine/cholesterol phase diagram: boundaries and composition of lipid rafts, *Biophys. J. 85*, 2406−2416.
16. Mannock, D. A., McIntosh, T. J., Jiang, X., Covey, D. F., and McElhaney, R. N. (2003) Effects of natural and enantiomeric cholesterol on the thermotropic phase behavior and structure of egg sphingomyelin bilayer membranes, *Biophys. J. 84*, 1038−1046.
17. Estep, T. N., Mountcastle, D. B., Barenholz, Y., Biltonen, R. L., and Thompson, T. E. (1979) Thermal behavior of synthetic sphingomyelin-cholesterol dispersions, *Biochemistry 18*, 2112−2117.
18. Estep, T. N., Freire, E., Anthony, F., Barenholz, Y., Biltonen, R. L., and Thompson, T. E. (1981) Thermal behavior of stearoylsphingomyelin-cholesterol dispersions, *Biochemistry 20*, 7115−7118.
19. Maulik, P. R., and Shipley, G. G. (1996) *N*-palmitoyl sphingomyelin bilayers: structure and interactions with cholesterol and dipalmitoylphosphatidylcholine, *Biochemistry 35*, 8025−8034.
20. Contreras, F. X., Sot, J., Ruiz-Arguello, M. B., Alonso, A., and Goñi, F. M. (2004) Cholesterol modulation of sphingomyelin activity at physiological temperatures, *Chem. Phys. Lipids 130*, 127−134.
21. Mattjus, P., and Slotte, J. P. (1996) Does cholesterol discriminate between sphingomyelin and phosphatidylcholine in mixed monolayers containing both phospholipids?, *Chem. Phys. Lipids 81*, 69−80.
22. Radhakrishnan, A., Li, X.-M., Brown, R. E., and McConnell, H. M. (2001) Stoichiometry of cholesterol-sphingomyelin condensed complexes in monolayers, *Biochim. Biophys. Acta 1511*, 1−6.
23. Veiga, M. P., Arrondo, J. L. R., Goñi, F. M., Alonso, A., and Marsh, D. (2001) Interaction of cholesterol with sphingomyelin in mixed membranes containing phosphatidylcholine, studied by spin-label ESR and IR spectroscopies. A possible stabilization of gel-phase sphingolipid domains by cholesterol, *Biochemistry 40*, 2614−2622.
24. Khelashvili, G. A., and Scott, H. L. (2004) Combined Monte Carlo and molecular dynamics simulation of hydrated 18:0 sphingomyelin-cholesterol lipid bilayers, *J. Chem. Phys. 120*, 9841−9847.
25. Untracht, S. H., and Shipley, G. G. (1977) Molecular interactions between lecithin and sphingomyelin. Temperature- and composition-dependent phase separation, *J. Biol. Chem. 252*, 4449−4457.
26. Smaby, J. M., Brockman, H. L., and Brown, R. E. (1994) Cholesterol's interfacial interactions with sphingomyelins and phosphatidylcholines: hydrocarbon chain structure determines the magnitude of condensation, *Biochemistry 33*, 9135−9142.
27. Guo, W., Kurze, V., Huber, T., Afdhal, N. H., Beyer, K., and Hamilton, J. A. (2002) A solid-state NMR study of phospholipid-cholesterol interactions: sphingomyelin-cholesterol binary system, *Biophys. J. 83*, 1465−1478.
28. Holopainen, J. M., Metso, A. J., Mattila, J.-P., Jutila, A., and Kinnunen, P. K. J. (2004) Evidence for the lack of a specific interaction between cholesterol and sphingomyelin, *Biophys. J. 86*, 1510−1520.
29. Slotte, J. P. (1995) Lateral domain heterogeneity in cholesterol/phosphatidylcholine monolayers as a function of cholesterol concentration and phosphatidylcholine acyl chain length, *Biochim. Biophys. Acta 1238*, 118−126.
30. Marsh, D. (1996) Lateral pressure in membranes, *Biochim. Biophys. Acta 1286*, 183−223.
31. Filippov, A., Oradd, G., and Lindblom, G. (2003) The effect of cholesterol on the lateral diffusion of phospholipids in oriented bilayers, *Biophys. J. 84*, 3079−3086.
32. Veiga, M. P., Goñi, F. M., Alonso, A., and Marsh, D. (2000) Mixed membranes of sphingolipids and glycerolipids studied by spin-label ESR spectroscopy. A search for domain formation, *Biochemistry 39*, 9876−9883.
33. Marsh, D., and Watts, A. (1982) Spin-labeling and lipid-protein interactions in membranes, in *Lipid-Protein Interactions* (Jost, P. C., and Griffith, O. H., Eds.) Vol. 2, pp 53−126, Wiley-Interscience, New York.
34. Lapidot, Y., Rappoport, S., and Wolman, Y. (1967) Use of esters of *N*-hydroxysuccinimide in the synthesis of *N*-acylamino acids, *J. Lipid Res. 8*, 142−145.
35. Barenholz, Y., and Gatt, S. (1982) Sphingomyelin: metabolism, chemical synthesis, chemical and physical properties, in *Phospholipids* (Hawthorne, A., Ed.) pp 129−177, Elsevier Biomedical Press, Amsterdam, London, and New York.
36. Marsh, D. (1981) Electron spin resonance: spin labels, in *Membrane Spectroscopy. Molecular Biology, Biochemistry and Biophysics* (Grell, E., Ed.) Vol. 31, pp 51−142, Springer-Verlag, Berlin, Heidelberg, and New York.
37. Marsh, D. (1989) Experimental methods in spin-label spectral analysis, in *Biological Magnetic Resonance* (Berliner, L. J., and Reuben, J., Eds.) Vol. 8, pp 255−303, Plenum Publishing Corp., New York.

38. Moser, M., Marsh, D., Meier, P., Wassmer, K.-H., and Kothe, G. (1989) Chain configuration and flexibility gradient in phospholipid membranes. Comparison between spin-label electron spin resonance and deuteron nuclear magnetic resonance, and identification of new conformations, *Biophys. J. 55*, 111−123.
39. Rama Krishna, Y. V. S., and Marsh, D. (1990) Spin label ESR and ^{31}P-NMR studies of the cubic and inverted hexagonal phases of dimyristoylphosphatidylcholine/myristic acid (1:2, mol/mol) mixtures, *Biochim. Biophys. Acta 1024*, 89−94.
40. Marsh, D. (1982) Electron spin resonance: spin label probes, in *Techniques in Lipid and Membrane Biochemistry* (Metcalfe, J. C., and Hesketh, T. R., Eds.) Vol. B4/II, pp B426/1−B426/44, Elsevier, Amsterdam.
41. Schorn, K., and Marsh, D. (1996) Lipid chain dynamics and molecular location of diacylglycerol in hydrated binary mixtures with phosphatidylcholine: spin label ESR studies, *Biochemistry 35*, 3831−3836.
42. Cevc, G., and Marsh, D. (1987) *Phospholipid Bilayers. Physical Principles and Models*, Wiley-Interscience, New York.
43. Vist, M. R., and Davis, J. H. (1990) Phase-equilibria of cholesterol dipalmitoylphosphatidylcholine mixtures—^{2}H nuclear magnetic-resonance and differential scanning calorimetry, *Biochemistry 29*, 451−464.
44. Ruocco, M. J., Siminovitch, D. A., Long, J. R., Das Gupta, S. K., and Griffin, R. G. (1996) ^{2}H and ^{13}C nuclear magnetic resonance study of *N*-palmitoylgalactosylsphingosine (cerebroside)/cholesterol bilayers, *Biophys. J. 71*, 1776−1778.
45. Veatch, S. L., and Keller, S. L. (2003) Separation of liquid phases in giant vesicles of ternary mixtures of phospholipids and cholesterol, *Biophys. J. 85*, 3074−3083.
46. Sankaram, M. B., and Thompson, T. E. (1991) Cholesterol-induced fluid-phase immiscibility in membranes, *Proc. Natl. Acad. Sci. U.S.A. 88*, 8686−8690.
47. Krasnowska, E. K., Bagatolli, L. A., Gratton, E., and Parasassi, T. (2001) Surface properties of cholesterol-containing membranes detected by Prodan fluorescence, *Biochim. Biophys. Acta 1511*, 330−340.
48. Veatch, S. L., and Keller, S. L. (2002) Organization in lipid membranes containing cholesterol, *Phys. Rev. Lett. 89*, 268101-1-268101-4.
49. Sachse, J.-H., King, M. D., and Marsh, D. (1987) ESR determination of lipid diffusion coefficients at low spin-label concentrations in biological membranes, using exchange broadening, exchange narrowing, and dipole−dipole interactions, *J. Magn. Reson. 71*, 385−404.

BI0474970